*Journal of Applied Fluid Mechanics*, Vol. 9, No. 5, pp. 2413-2425, 2016.
Available online at www.jafmonline.net, ISSN 1735-3572, EISSN 1735-3645.
DOI: 10.18869/acadpub.jafm.68.236.25942

# Effects of Heavy Fuel Oil Blend with Ethanol, n-Butanol or Methanol Bioalcohols on the Spray Characteristics

P. Ghadimi† and H. Nowruzi

*Department of Marine Technology, Amirkabir University of Technology, Tehran,* Tehran 14717, Iran

†*Corresponding Author Email: pghadimi@aut.ac.ir*

(Received November 29, 2015; accepted December 28, 2015)

## ABSTRACT

Blending of fossil fuels with alcohols is one of the most impressive strategies for emission control and enhancement of fuel efficiency. Accordingly, in the current paper, the effects of blend of Heavy Fuel Oil (HFO) with bioalcohols are numerically studied on the non-reacting spray characteristics. Three different fuels are considered by mixture of HFO with 20% of n-Butanol, Ethanol, and Methanol and compared against Pure HFO. For this purpose, the microscopic and macroscopic spray characteristics of the blended fuels are evaluated through the investigation of spray penetration, cone angle, spray volume, and Sauter Mean Diameter (SMD). Moreover, for detailed understanding of the spray characteristics, the non-dimensional numbers of Weber and Ohnesorge, and liquid spray morphology are analyzed. Also, the study of Histogram of density and droplet diameter is conducted. Eulerian-Lagrangian multiphase scheme is used for simulation of air-fuel interaction in OpenFOAM CFD toolbox. Lagrangian Particle Tracking method is utilized for fuel droplet tracking in Lagrangian scheme. A hybrid breakup model of KH-RT and standard model of k-ε in RANS is used respectively for breakup and turbulence modeling. The obtained numerical results are validated against existing experimental data with suitable accordance. Based on the computational results, longer spray penetration length, larger spray cone angle and greater spray volume are achieved for the blended fuels. It was also concluded that HFO-Ethanol improves the macroscopic characteristics compared to two other blended fuels, albeit the effect is very minimal. In addition, lower SMD value is obtained for the blended fuels compared to pure HFO.

**Keywords**: Non-reacting; Spray characteristics; OpenFOAM; HFO-bioalcohols blend; Computational fluid Dynamic.

## NOMENCLATURE

| | | | |
|---|---|---|---|
| $a$ | acceleration of droplet in the interface | $\mathrm{Re}_l$ | liquid Reynolds number |
| *ASOI* | after start of injection | *RMSE* | root mean square error |
| $D_d$ | diameter of fuel droplet | $r_0$ | droplet radius before breakup |
| $f_{co}$ | effects of collision of the droplets | *SMD* | sauter mean diameter |
| $f_{bu}$ | effects of droplets breakup | *SIMPLE* | semi implicit method for pressure linked equations |
| *HFO* | heavy fuel oil | $T$ | Taylor number |
| *LPT* | lagrangian particle tracking | $T_{amb}$ | ambient temperature |
| *Oh* | Ohnesorge number | $u_{rel}$ | relative speed between droplets and ambient gas |
| $p_b$ | chamber pressure | $We_g$ | gas Weber number |
| $p_{inj}$ | injection pressure | $We_l$ | liquid Weber number |
| Pr | Prandtl number | x $r_c$ | radius of child droplets |
| *PM* | particulate matter | | |
| *RANS* | Reynolds averaged Navier Stokes | | |

| | |
|---|---|
| $\nu_g$ | gas kinematic viscosity |
| $\Lambda_{KH}$ | kelvin-Helmholtz wavelength |
| $\Omega_{KH}$ | kelvin-Helmholtz growth rate |
| $\Lambda_{RT}$ | rayleigh-Taylor wavelength |
| $\Omega_{RT}$ | rayleigh-Taylor growth rate |
| $\mu$ | dynamic viscosity |
| $\rho_l$ | liquid density |
| $\rho_g$ | gas density |
| $\tau_{bu}$ | breakup time |
| $\omega$ | surface tension |
| $\sigma$ | instability wave growth rate |

## 1. INTRODUCTION

Heavy Fuel oils (HFO) as the main fuels in large diesel engines are considered very attractive because of their low price. Accordingly, several studies have been recently conducted to investigate the combustion, atomization procedure, and spray characteristics of HFO (Fink *et al*. 2008; Kyriakides *et al*. 2009; Struckmeier *et al*. 2009; Cordtz *et al*. 2014; Stamoudis *et al*. 2014). However, due to low quality of this reference fuel, high levels of NOx and PM emissions are apparent from diesel engines exhaust. These emissions cause air and water pollutions and this issue has attracted special attentions of the international community and governments to control the resulting environmental pollutions. Based on these concerns, researchers are consistently looking for solutions to simultaneously decrease the emissions and improve the fuel efficiency (Zoulalian 2010). Addition of alcohols including butanol, ethanol, and methanol to the base fuel is one of the appealing solutions and several studies have been presented that deal with the blend of butanol, ethanol and methanol with fossil fuels.

Remarkable interests related to study on the butanol-diesel blend are observed based on the Scopus database (Nowruzi *et al*. 2014). One such study is the work of Rakopoulos *et al*. (2010). In this work, they investigated the influence of using blended fuels on the level of emissions. Their considered fuels included 8%, 16% and 24% of normal butanol (n-butanol) with conventional diesel fuel. They detected a reduction in CO and NOx and enhancement of HC by an increase in volumetric percentage of n-butanol. Yao *et al*. (2010) experimentally studied the effect of diesel/n-butanol fuels and triple injection strategy on the emissions and performance of large diesel engine. Their results indicated an improvement on soot, CO and NOx emissions by addition of n-butanol to the diesel fuel. Karabektas and Hosoz (2009) showed that addition of iso-butanol increases the hydrocarbon while CO and NOx are decreased. The influence of using diesel/ n-butanol fuel blends on the performance of a small diesel engine and its emissions is studied by Dogan (2011). In their work, they found that by utilizing diesel/ n-butanol fuel, smoke, CO, and NOx are decreased and hydrocarbon is increased. In addition, a decrease in PM was reported by Zhang and Balasubramanian (2014) by using 5%, 10%, 15% and 20% of butanol blend with ultra low sulfur diesel in a non-road diesel engine.

In the meantime, another alcohol for addition with conventional fuels is methanol. Song *et al*. (2008) studied the influence of methanol on emission, combustion and performance of dual-fuel engine. They showed that by methanol addition to the base fuel, better fuel economy, notable reduction of smoke emissions, average decrease of NOx, and increase of HC and CO are achieved. Sayan *et al*. (2010) also conducted a study on the influence of injection pressure and timing on the performance and emission properties of a single cylinder diesel engine fueled by methanol-diesel. They found an increase in NOx and a decrease in CO and HC by enhancement of volume of methanol in the blend. Also, emissions and combustion characteristics of a diesel engine fueled with diesel-methanol were studied by Canakci *et al*. (2008). In this regard, the influences of injection timing on the emissions of a diesel engine using diesel–methanol are also probed Sayin *et al*. (2009). Furthermore, the influences of methanol fumigation on engine performance and emissions were studied by Zhang *et al*. (2011).

Another popular alcohol for adding to the basic fuels is ethanol and some important studies have been conducted about the fossil-ethanol blended fuels in diesel engines. Park *et al*. (2010) investigated the emission and combustion properties of different bioethanol-diesel blends. Enhancement of the ignition delay due to the low cetan number and decrease of gas temperature were observed by increasing the bioethanol in the blend. Can *et al*. (2004) studied the effect of 10% and 15% by volume of ethanol in diesel fuel on the engine emissions under different injection pressures. The influences of ethanol fumigation on the emissions and performance were investigated by Tsang *et al*. (2010) and Chauhan *et al*. (2011). Also, the effect of biodiesel-ethanol blend on the spray characteristics was studied by Yoon *et al*. (2011) for a single cylinder common-rail diesel engine. Their results showed that by using biodiesel-ethanol blended fuel, the SMD decreases, while relative velocity between the injected fuel and the ambient gas increases. In addition, the effect of two-stage injection pressure and exhaust gas recirculation on the spray behavior and emission characteristics of diesel-ethanol fuel blends in diesel engine is studied by Park *et al*. (2010). They used spray tip penetration, and spray cone angle for evaluation of spray development process. Recently, strong effect of the fuel type on spray properties has been presented by Behringer (2014) using 25 % ethanol and 16 % or 25 % butanol blend with the reference

fuels. Higher droplet size of the blended fuels compared to basic fuel was one of his results.

Experimental researches are expensive or difficult to conduct, especially for heavy duty diesel engines. Therefore, CFD method is considered as an attractive alternative for the experimental research in the field of diesel engine. Several commercial software such KIVA, STAR-CD, and AVL FIRE have been developed for studying injection and combustion in diesel engines. Also, many studies related to HFO injection have been conducted by these softwares (Kyriakides *et al*. 2009; Struckmeier *et al*. 2009; Wang *et al*. 2014; Andreadis *et al*. 2011). Despite of these software, open source CFD toolboxes such as OpenFOAM are currently more attractive in the field of fuel injection research. Therefore, many studies related to fuel injection have been recently conducted by OpenFOAM (Gjesing *et al*. 2009; Kassem *et al*. 2011; Ismail *et al*. 2013; Yousefifard *et al*. 2014, 2015). Accordingly, in the present study, the open source CFD toolbox of OpenFOAM is utilized for modeling the described blended fuels injection.

The impact of physical characteristics of the injected fuels on fundamental properties of the resulting spray is undeniable, and hence; their investigation seems to be imperative. However, based on the cited works, there looks to be a lack of study on the spray characteristics of HFO-bioalcohols blends. For this reason, in the present study, a numerical study is conducted on the spray characteristics of HFO blend with 20% of different alcohols including normal butanol, ethanol or methanol. This study is performed under non-reacting condition. For evaluation of the fuel spray properties, different non-dimensional numbers and liquid spray morphology are analyzed. In addition, after probing into the histogram of density and droplet diameter, microscopic and macroscopic characteristics of the blended fuels are investigated. For this purpose, liquid spray penetration length, spray cone angle, sprays volume and sauter mean diameters (SMD) are examined.

## 2. HEAVY FUEL OIL WITH BIOALCOHOLS OF N-BUTANOL, ETHANOL OR METHANOL AS BLENDED FUELS

Nowadays, the use of alcohols such as n-butanol, ethanol and methanol in the internal combustion engines is of great interest. In the meantime, the blends of alcohols with HFO leading to green fuel are considered significant potential for reducing pollution. However, their influence on the spray characteristics is not well known. In this context, physical properties of the considered alcohols in relation to combination with HFO are explained below.

A four carbon atom structure alcohol that can be produced by petrochemical processing from oil sources or as a renewable fuel from biomass is butanol. This alcohol due to the position of the hydroxyl group has four isomers including n-butanol (CH3 CH2 CH2 CH2 OH), 2-butanol (CH3 CH2 CHOHCH3), i-butanol ((CH3)2 CH2 CHOH) and t-butanol ((CH3)3 COH). These isomers with different molecular structures reveal different properties. N-butanol has a higher density, flash, and boiling points in comparison with other isomers. Consequently, biomass based n-butanol is the selected isomer for blending with HFO in the current study.

A one carbon atom alcohol with simplest molecular structure is methanol. The molecular structure of this alcohol is (CH3 OH). This alcohol is hygroscopic and can absorb vapor from the atmosphere. Therefore, water absorption and phase separation of methanol is observable in HFO–methanol blended fuel. Methanol can be extracted from the destructive distillation of wood and is therefore named as wood alcohol. However, methanol is nowadays produced from the synthetic gas or biogas (in a catalytic industrial process directly from the carbon monoxide, carbon dioxide, and hydrogen). Despite of this, the sustainable technologies for producing methanol from biomass are currently economically unfeasible.

On the other hand, ethanol with molecular structure of (CH3 CH2 OH) is a two carbon ethyl alcohol. Currently, ethanol is considered as one of the most interesting alcohol-based fuel. This alcohol is extracted from the simple fermentation of natural sugars, starches, or cellulosic biomass (Kumar *et al*. 2013).

A comparison of the physicochemical characteristics of biomass based n-butanol, ethanol, and methanol can be discussed based on six criteria. These characteristics are Hydroscopicity, Flash Point, Energy Density, Cetan Number, Hydrocarbon Chain, and Kinematic Viscosity. The Hydroscopicity of n-butanol is lower than ethanol and methanol. Therefore, n-butanol is less affected by the climate change. On the other hand, flash point of n-butanol has higher value than two other alcohols and thus more safe compared to the other two types of alcohol. Higher energy density of butanol leads to generation of about 25% more energy than methanol and ethanol. Formation of a more uniform combustion is a result of higher quantity of Cetan Number in n-butanol. Also, due to larger Hydrocarbon chain in butanol, it is fairly non-polar and more similar to diesel fuels. On the other hand, higher comparative value of kinematic viscosity is evident for n-butanol compared to other alcohols (Kumar *et al*. 2013).

Molecular structure and schematic of n-butanol, ethanol and methanol compared to HFO (approximated by C14H30) are presented in Fig. 1. Heavy fuel oil with straight linear hydrocarbon chain shows higher miscibility with the considered alcohols. Therefore, one may conclude that blended fuels including HFO-normal butanol, HFO-ethanol, and HFO-methanol are appropriate alternative fuels. Accordingly, non-reacting spray characteristics of these blended fuels are considered for the present study. For numerical simulation of these blended fuels, their physicochemical properties are applied

to OpenFOAM. Therefore, thermo-physical properties of fuel component are calculated and tabulated in the Fuel Library of OpenFOAM software. Fundamental characteristic of the modeled HFO and n-butanol, ethanol, or methanol are presented in Table 1.

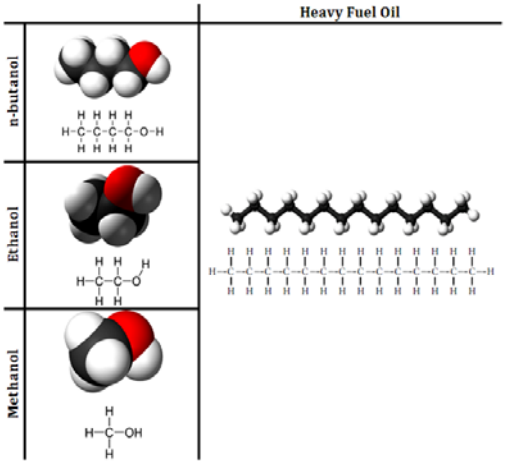


**Fig. 1. Molecular structure and sketch map of n-butanol, ethanol, and methanol compared to C14H30 as a Heavy Fuel Oil.**

Also, as pointed out earlier, 20% (volumetric percentage) of n-butanol or 20% of ethanol, or 20% of methanol is utilized for blending with HFO (Table 2).

**Table 1 Physical characteristics of HFO, n-butanol, ethanol, and methanol**

| Physical Characteristics | Density ( $Kg / m^{-3}$ ) | Viscosity ( $m^2 s^{-1}$ ) | Surface Tension ( $Nm^{-1}$ ) |
|---|---|---|---|
| Heavy Fuel Oil | 895 | 1.2 e-5 | 0.029 |
| n-Butanol | 810 | 3.19 e-6 | 0.024 |
| Ethanol | 785 | 1.40e-6 | 0.0219 |
| Methanol | 786 | 7.04 e-7 | 0.0225 |

**Table 2 Volumetric percentage of alcohols and basic fuel**

| Blended fuels | Volumetric percentage in blended fuel | | | |
|---|---|---|---|---|
| | HFO | n-butanol | Ethanol | Methanol |
| Pure HFO | 100% | 0% | 0% | 0% |
| HFO-normal Butanol | 80% | 20% | 0% | 0% |
| HFO-Ethanol | 80% | 0% | 20% | 0% |
| HFO-Methanol | 80% | 0% | 0% | 20% |

It must also be noted that these fuel physical characteristics are temperature dependent.

## 3. NUMERICAL METHODOLOGY

### 3.1. SIMULATION OF SPRAY BREAKUP

Structure of the liquid fuel spray is a complex phenomenon and the mechanism of fuel spray atomization and breakup is not well understood. However, it is generally accepted that injected liquid fuel spray into the air medium of the combustion chamber has three main regions. These regions are atomization, dense spray, and dilute spray regions. In an atomization region, blobs, ligaments, and droplets are observable. However, due to the primary breakup procedure, decomposition of the blobs to ligaments and similarly ligaments disintegration to the droplets happen in the dense spray region. Consequently, an area of fully spherical droplets becomes apparent in the dilute region at the end of the liquid spray structure (Jiang *et al*. 2010). As a result, primary and secondary breakup modeling is the principal foundation in the liquid spray simulation.

For primary breakup modeling, the initial droplets radius and spray angle are considered as an initial conditions for the secondary breakup. In other words, the distinction between atomization and droplets breakup is neglected. This is attributed to the high pressure and fuel density around the injector nozzle. Common approach for the primary breakup with this sort of assumption is the blob method that was presented by Reitz and Diwakar (Reitz and Diwakar 1986, 1987). A schematic of the blob method can be seen in Fig. 2.

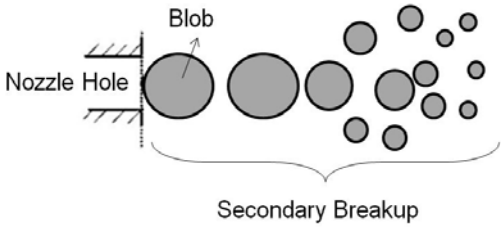


**Fig. 2. Blob method.**

In the secondary breakup of the core of the liquid fuel, due to aerodynamic force on the fuel droplet, decomposition of the primary droplet into minor parcels occurs. This aerodynamic force is formed by the relative velocity ( $u_{rel}$ ) between the injected liquid fuel and the present ambient gas in the combustion chamber. Based on this force, instabilities grow on the liquid fuel surface. Due to these instabilities, liquid fuel breakup becomes apparent. According to the term of surface tension in the Weber number of the gaseous phase, a resistive force is detectable for maintaining the spherical shape of droplet. The Weber number of the gaseous phase is defined in as

$$We_g = \frac{\rho_g u_{rel}^2 D_d}{\sigma} \quad (1)$$

where $D_d$ is the diameter of a fuel droplet.

Two different secondary breakup regimes are provided by Reitz and Diwakar based on the Weber number (Reitz and Diwakar 1986, 1987). However, in the current study, due to the remarkable potential of the hybrid breakup model for the secondary breakup modeling (Ghasemi *et al*. 2012), the KH-RT model is utilized. A schematic of the KH-RT breakup model is presented in Fig. 3. In the KH-RT breakup model, KH and RT instabilities are considered. KH model is used near the injector nozzle and RT is utilized at a particular distance from the nozzle (Hwang *et al*. 1996). This is mainly due to the fact that a rapid decrement of the droplet diameter is observable close to the injector nozzle for the RT model.

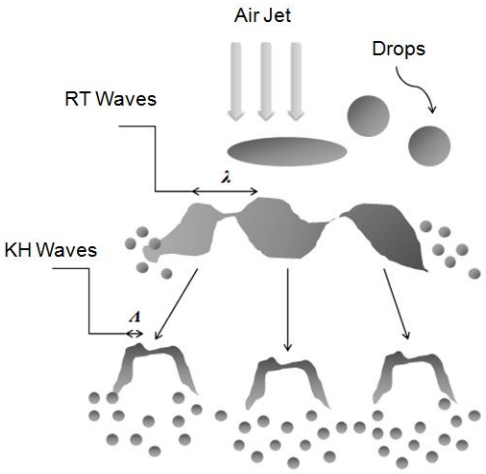


**Fig. 3. Schematic of the KH-RT Breakup model.**

As pointed out earlier, the KH-RT scheme is a combination of KH and RT models. In the KH model, growth of Kelvin–Helmholtz instability on the cylindrical liquid jet surface with primary radius of $r_0$ occurs. This model was presented by Reitz (1987). Formation of the spectrum of sinusoidal surface waves on the surface of a liquid fuel is the basic assumption of the KH model. Turbulence in the injector nozzle hole and relative speed between the liquid droplets and ambient gas ($u_{rel}$) are the reasons for the formation of these instabilities. Wavelength ($\Lambda_{KH}$) and growth rate ($\Omega_{KH}$) of the fastest growing wave on the surface of the liquid jet in a KH model are as follows:

$$\Omega_{KH}\left[\frac{\rho_l r_0^3}{\sigma}\right]^{0.5} = \frac{0.34 + 0.38 \cdot We_g^{1.5}}{(1+Oh)(1+1.4 \cdot T^{0.6})} \quad (2)$$

$$\frac{\Lambda_{KH}}{r_0} = 9.02 \frac{(1+0.45 \cdot Oh^{0.5})(1+0.4 \cdot T^{0.7})}{(1+0.865 \cdot We_g^{1.67})^{0.6}} \quad (3)$$

where $Oh$ and $T$ are dimensionless numbers of Ohnesorge and Taylor, respectively which are defined as

$$Oh = \frac{\sqrt{We_l}}{\mathrm{Re}_l}$$

$$T = Oh\sqrt{We_g}$$

$$We_g = \frac{\rho_g u_{rel}^2 r_0}{\sigma}$$

$$We_l = \frac{\rho_l u_{rel}^2 r_0}{\sigma} \quad (4)$$

Rate of change of the droplet radius in the KH model and the dimensionless time of breakup or characteristics breakup time are:

$$\frac{dr}{dt} = -\frac{r_0 - r_c}{\tau_{bu}} \quad (5)$$

$$\tau_{bu} = 3.788 \cdot B_1 \frac{r_0}{\Lambda_{KH} \cdot \Omega_{KH}} \quad (6)$$

Radius of the new droplet is determined as follows:

$$r_c = B_0 \cdot \Lambda_{KH} \quad (7)$$

KH breakup is applicable, when

$$B_0 \cdot \Lambda_{KH} \le r_0 \quad (8)$$

Another instability in the KH-RT hybrid breakup model is called Rayleigh–Taylor (RT) instability. RT instability is the result of denser fluid inertia against the system acceleration. According to Bellman and Pennington (1954) study, growth rate of the fastest growing wave and the corresponding wavelength in RT model are

$$\Omega_{RT} = \sqrt{\frac{2}{2\sqrt{3\sigma}} \frac{[a(\rho_l - \rho_g)]^{3/2}}{\rho_l + \rho_g}} \quad (9)$$

$$\Lambda_{RT} = C_3 2\pi \sqrt{\frac{3\sigma}{a(\rho_l + \rho_g)}} \quad (10)$$

Computational procedure and validation of the proposed model are presented, next.

## 4. COMPUTATIONAL MODEL

### 4.1 Computational Procedure

The Eulerian-Lagrangian multiphase scheme is

employed for modeling of the interaction of liquid fuel and gaseous medium in the combustion chamber. Continuous air phase is analyzed by five partial differential equations in the Eulerian scheme. These five equations include continuity equation, conservation of energy, and momentum conservation equations (in three directions). Detailed information of these equations has been presented by Nowruzi *et al*. (2014). Finite volume method (FVM) and SIMPLE algorithm are implemented for discretization of the governing equations and the velocity-pressure coupling in OpenFOAM, respectively.

In the present paper, the standard K-ε turbulence model in the unsteady RANS method is applied. Lower computational cost and sufficient accuracy is the reasons for selecting this turbulence model (Jiang *et al*. 2010). Time step for the current study is considered to be $1.0 \times 10^{-6}\ s$ .

Lagrangian approach is utilized for prediction of the droplets behavior. Lagrangian particle tracking (LPT) technique is applied for computing the non-spherical particles orientation and the rate of rotation. For this purpose, Eq. (11) is used as spray equation which defines the probability in the condition space of the randomized variables.

$$\frac{\partial f}{\partial t} + \nabla_x \cdot (fu) + \nabla_v \cdot \left( f \frac{\partial u}{\partial t} \right) + \frac{\partial}{\partial r}\left( f \frac{\partial r}{\partial t} \right) + \frac{\partial}{\partial T}\left( f \frac{\partial T}{\partial t} \right) + \frac{\partial}{\partial y}\left( f \frac{\partial y}{\partial t} \right) + \frac{\partial}{\partial \dot{y}}\left( f \frac{\partial \dot{y}}{\partial t} \right) = f_{co} + f_{br} \tag{11}$$

Probable number of the droplets per unit volume is expressed by the term $f(X, V, r, T_d, T, y, \dot{y}, t)$ . Also, the influences of collision of the droplets and droplets breakup are considered in Eq. (11) as source terms

## 4.2 Grid Generation and Validation Study

Due to lack of any experimental data for the spray characteristics of HFO-alcohols blends under non-reacting conditions, a grid resolution sensitivity analysis for HFO is performed. This analysis is conducted under injection pressure of 100 MPa. Afterward, based on a proper mesh structure, the numerical results of the penetration length and spray cone angle of HFO are validated against an experimental data (Fink *et al*. 2008). The experimental setup of the selected study for validation analysis is illustrated in Table 3.

Four different fully structured meshes are considered to study the grid resolution sensitivity. These meshes are formed from the coarse mesh resolution (0.004m) to fine mesh resolution (0.001m) as presented in Fig. 4. Based on Fig. 4, mesh structure with resolution of 0.00133m are selected as an appropriate grid for the validation study. Subsequently, based on the mesh structure of Fig. 5, numerical results of the spray penetration length and spray cone angle of HFO are compared against the experiment (Fink *et al*. 2008). Based on Fig. 5, the RSME of the penetration length and spray cone angle at the injection pressure of 100 MPa are 3.21 and 2.34, respectively.

**Table 3 Experimental setup of validation study**

| Model Parameter | |
|---|---|
| Combustion Chamber | Chamber backpressure = 1.4 MPa |
| | Ambient temperature = 298 K |
| Injection Parameters | Common-rail high pressure injection |
| | Hydro-mechanical injector |
| | Eight nozzle holes with a diameter = 0.27mm |
| | Injection up to 5000 mg/str |
| | Fuel injection pressure of 60 and 100 MPa |
| | Injection total mass = 34 mg |
| Measurement Technique | scatter light technique of Mie-scatter |

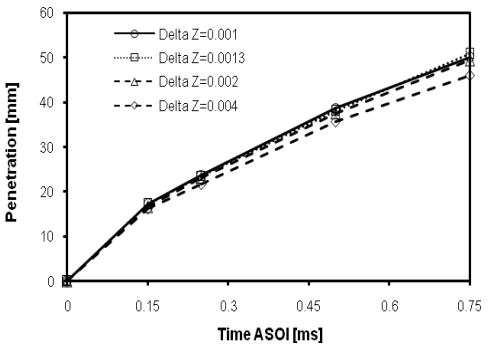


**Fig. 4. Grid independency test of the HFO spray penetration length at the injection pressure of 100 MPa.**

To ensure the suitability of the selected model for modeling alcohols, a grid resolution sensitivity analysis is also performed for butanol. Accordingly, the grid independency test for penetration length of butanol under injection pressure of 72 MPa is presented in Fig. 6. Then, based on the proper mesh structure of (0.00133m) in Fig. 7, the numerical results of penetration length are validated against the results of Reddemann *et al*. (2009). As evident in Fig. 7, a suitable accordance is observed between numerical result and experimental data with a RSME of 1.09.

## 4.3 Model Specifications

Injection setup and combustion chamber specifications for the current study are presented in Table 3. As evident in Table 4, constant volume combustion chamber and a single hole injector are selected. To calculate the injection mass flow rate, Pickett *et al*. (2013) scheme is applied to the OpenFOAM CFD toolbox.

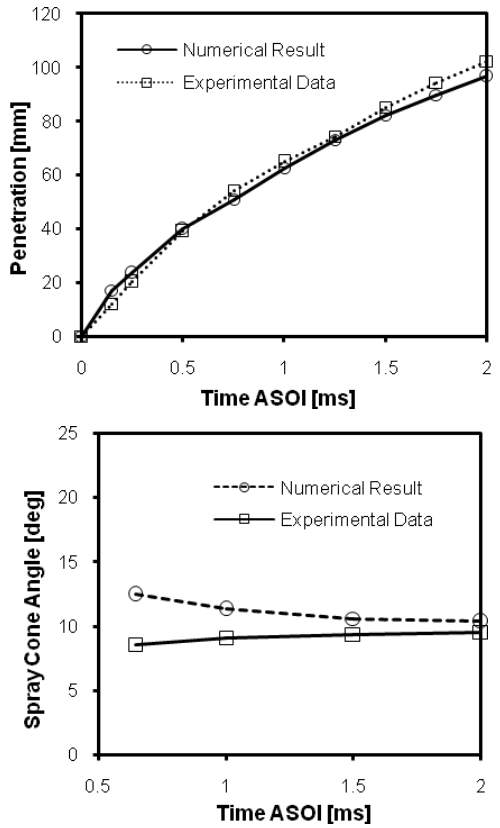


**Fig. 5. Comparison of the numerical and experimental spray penetration length and spray cone angle of HFO at the injection pressure of 100 MPa (Fink *et al*. 2008).**

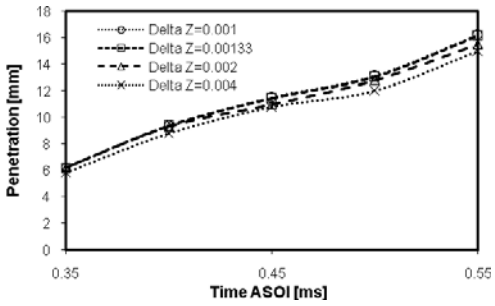


**Fig. 6. Grid independency test for the butanol spray penetration length at the injection pressure of 72 MPa**.

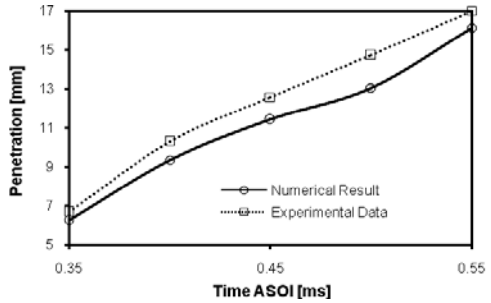


**Fig. 7. Comparison of the numerical and experimental spray penetration length of butanol at the injection pressure of 72 MPa (Reddemann *et al*. 2009).**

**Table 4 Combustion chamber and injection setup**

| Model Parameter | | Value |
|---|---|---|
| Combustion Chamber Parameters | Length (mm) | 450 |
| | Diameter (mm) | 150 |
| | Backpressure (MPa) | 1.4 |
| | Ambient temperature (K) | 298 |
| Injection Parameters | Nozzle diameter (mm) | 0.27 |
| | Fuel injection pressure (MPa) | 100 |
| | Injection total mass (mg) | 34 |

The structure of the computational mesh is displayed in Fig. 8. Based on Fig. 8, a fully structured mesh is utilized for the current study.

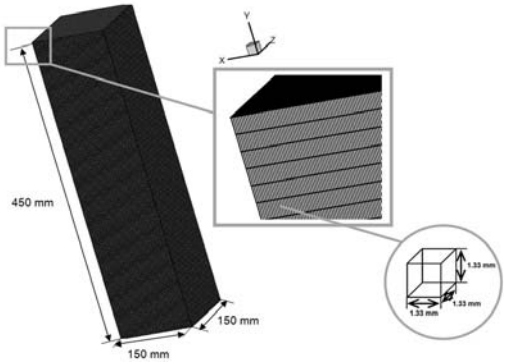


**Fig. 8. Structure of the computational mesh.**

Microscopic and macroscopic computational results of the non-reacting spray properties of HFO blend with n-butanol, ethanol, or methanol are presented, next.

## 5. RESULTS AND DISCUSSION

### 5.1 Analysis on the Non-Dimensional Number

Physical characteristic of the injected fuel is one of the main influential factors on the liquid spray behavior. Non-dimensional numbers are favorable criteria for better investigations of these physical properties.

Two prominent dimensionless numbers in this context are Weber (We) and Ohnesorge (Oh) numbers. Weber number is a relation between the fluid inertia and surface tension. On the other hand, Ohnesorge is defined as a viscous force to inertia and surface tension. Relation between Weber and Ohnesorge number for all liquid droplets of HFO-normal Butanol, HFO-Ethanol, and HFO-Methanol is illustrated at 1.5 ms after start of injection in Figs. 9 through 11, respectively.

As evident in Figs. 9 through 11, few points of Ohnesorge Number are observed that are far away from the cloud. These points represent the spray particles that have lower diameter. Therefore, they have higher Ohnesorge Number. On one hand,

some particles have significant lower diameter at the end of the breakup procedure compared to the other particles. On the other hand, based on the Reynolds formula ( $\mathrm{Re} = u_{rel}.\mathrm{D_d}/v$ where $\mathrm{D_d}$ is droplet diameter), these particles have notable lower Reynolds number. As a result, based on the Ohnesorge formula (Eq. (4)), these spray particles have significant higher Ohnesorge number due to their lower Reynolds number.

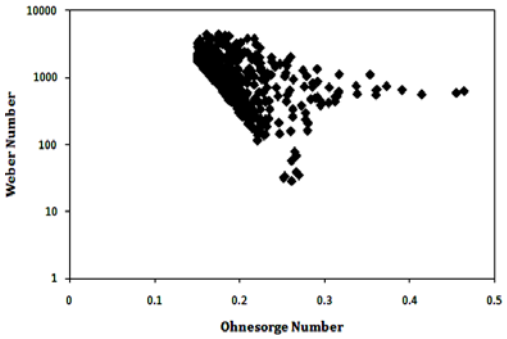


**Fig. 9. Weber number Vs Ohnesorge number for HFO-Butanol at 1.5ms ASOI (Pinj=100 MPa, Pback=1.4MPa, Tamb=298K).**

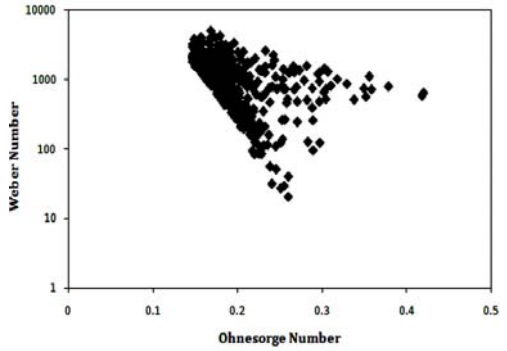


**Fig. 10. Weber number Vs Ohnesorge number for HFO-Ethanol at 1.5ms ASOI (Pinj=100 MPa, Pback=1.4MPa, Tamb=298K).**

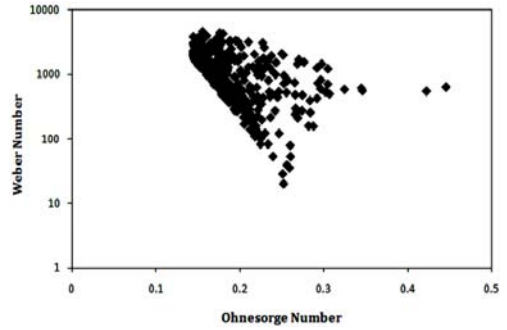


**Fig. 11. Weber number Vs Ohnesorge number for HFO-Methanol at 1.5ms ASOI (Pinj=100 MPa, Pback=1.4MPa, Tamb=298K).**

On the other hand, based on Figs. 9 through 11, maximum of Weber number related to HFO-Ethanol is negligibly higher than that of HFO-Methanol. Similarly, maximum of Weber number related to HFO-Methanol is a little higher value than that of HFO-normal butanol. Therefore, it can be concluded that higher comparative value of Weber number related to HFO-Ethanol is indicative of its lower surface tension compared to those of other blended fuels. However, the minimum Weber number related to HFO-Ethanol is less than that of HFO-Methanol. Similarly, minimum Weber number related to HFO-Methanol is less than that of HFO-normal butanol.

On the other hand, there appears to be a slight relocation of the resulting cloud related to Ohnesorge number of HFO-Ethanol in comparison with that of HFO-Methanol. In addition, a larger Ohnesorge number is evident for HFO-normal butanol. Based on this observation, one may conclude that HFO-normal butanol is more influenced by viscosity due to its larger Ohnesorge number.

To better compare the non-dimensional numbers of Webber and Ohnesorge for different blended fuels, the maximum and minimum of these numbers for different blended fuels are presented in Table 5.

**Table 5 Maximum and Minimum of Webber and Ohnesorge numbers for HFO-normal Butanol, HFO-Ethanol and HFO-Methanol**

| Blended fuels | Webber number | | Ohnesorge number | |
|---|---|---|---|---|
| | Min. | Max. | Min. | Max. |
| HFO-normal Butanol | 28.5 | 9352.59 | 0.1485 | 0.4783 |
| HFO-Ethanol | 18.17 | 9484.22 | 0.1453 | 0.4260 |
| HFO-Methanol | 18.29 | 9453.66 | 0.1425 | 0.4522 |

## 5.2 Liquid Spray Morphology

Various physical characteristics of the injected fuel would result in different liquid spray structures during the start of injection into the combustion chamber. Therefore, a morphology study of the liquid spray structures of different blended fuels is presented in Fig. 12.

Based on Fig. 12, it can be observed that the tip of the liquid spray becomes sharper during the injection to the combustion chamber for all three blended fuels, especially after 0.5 ms ASOI. This phenomenon can be attributed to the influence of induced air motion on the liquid spray structure (Yousefifard *et al*. 2014). Also, general appearance of the spray structure is approximately similar for all three blended fuels. However, a negligible fattest spray structure is detectable for the HFO-Ethanol.

For a more detailed illustration, the liquid spray structures of three different blended fuels in comparison with pure HFO are displayed in Fig. 13. According to Fig. 13, sharper tip in the greater spray structure is apparent for the liquid spray structures of the blended fuels as opposed to the pure HFO, at 1.5ms ASOI.

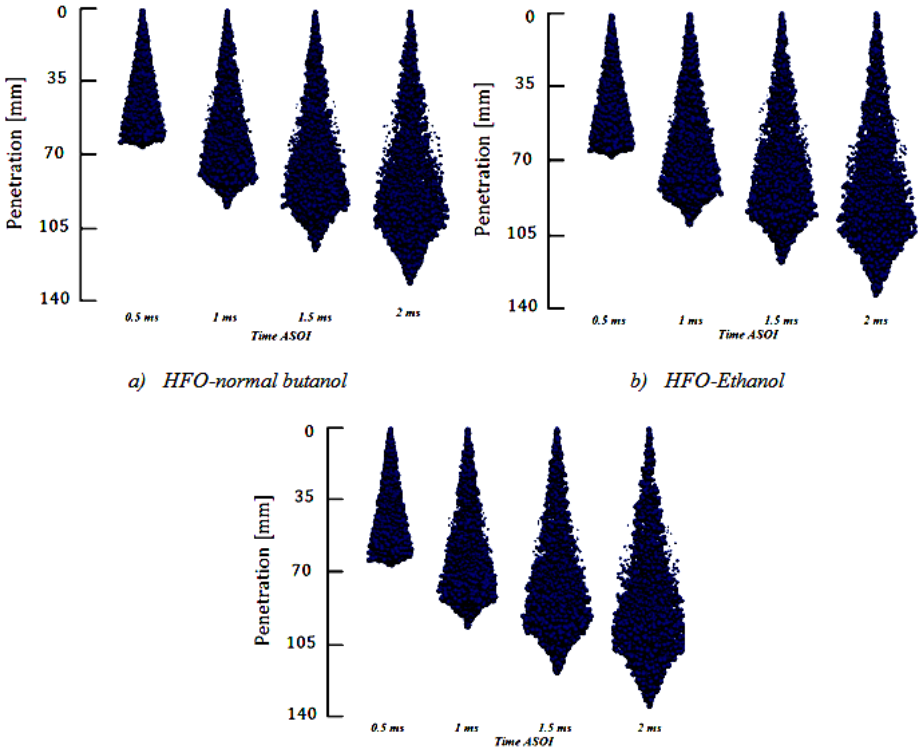


**Fig. 12. Liquid sprays structures for different blended fuels during the injection timeline.**

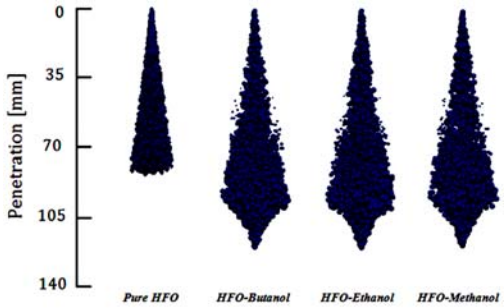


**Fig. 13. Liquid sprays structures of the blended fuels compared to pure HFO at 1.5ms ASOI.**

On the other hand, as shown in Fig. 13, liquid fuel jet returns from the lateral edges of spray for all the blended fuels. This is due to the difference in fluid properties between the blended fuels and pure HFO (Sepret *et al*. 2010).

## 5.3 Analysis of the Histogram Data

Histograms illustrate the distribution of the considered data, and probability distribution of the continuous variables can be extracted from them. Histogram of the density for HFO-normal Butanol, HFO-Ethanol, and HFO-Methanol at 1.5ms ASOI is presented in Fig. 14. As evident in this figure, number of observed data that fall on the interval surrounding the density distribution of 895 Kg.m-3 is larger than other intervals for all three different fuels. Also, density distributions are more frequent for all three blended fuels in the range of 885 Kg.m-3 to 905 Kg.m-3. Moreover, a fluctuation on the frequency of density distribution is observed after 905 Kg.m-3 for HFO-normal Butanol.

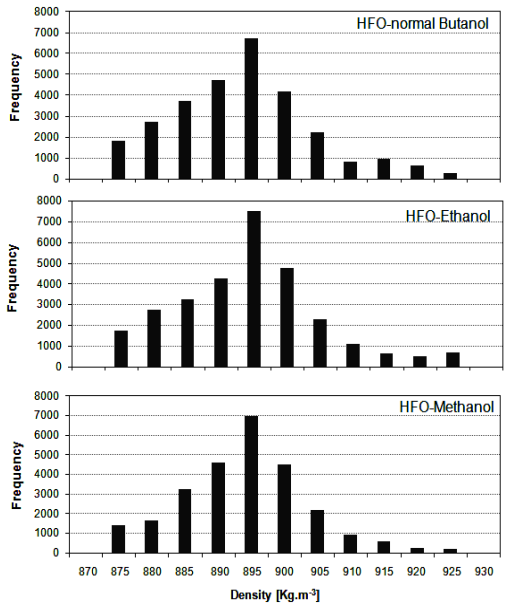


**Fig .14. Histogram of density for HFO-normal Butanol, HFO-Ethanol, and HFO-Methanol at 1.5ms ASOI.**

Histogram of the particle diameter for HFO-Butanol, HFO-Ethanol, and HFO-Methanol at 1.5ms ASOI is presented in Fig. 15. Based on Fig.

15, the highest frequency in droplet diameter distribution is observed in an interval surrounding 20 micron for all three blended fuels. This implies that the mean value of the droplets diameter from the secondary breakup (until 1.5 ms ASOI later) is in approximately 20 micron. Also, one can be observe that lower distribution frequency is apparent in the interval of 40 micron. Higher frequency in the interval of 10 micron for the HFO-methanol represents an improvement of the breakup procedure for this fuel compared to the other two blended fuels. Indeed, lower viscosity and surface tension of HFO-Methanol compared to two other blended fuels, improves the atomization procedure (Lefebvre 1989). Moreover, no droplet samples are displayed for droplet diameter greater than 40 micron.

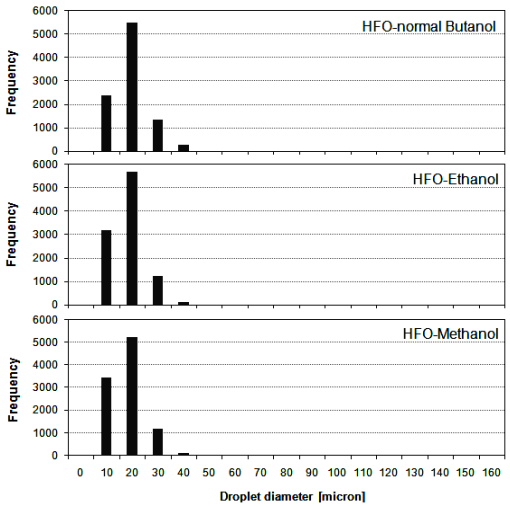


**Fig. 15. Histogram of the particle diameter for HFO-normal Butanol, HFO-Ethanol, and HFO-Methanol at 1.5ms ASOI.**

## 5.4 Analysis on Macroscopic and Microscopic Properties

Liquid spray structure has particular macroscopic and microscopic properties. These properties are used for evaluation of the liquid spray behavior. Spray penetration length, spray cone angle, and spray volumes are the main macroscopic properties of the liquid spray. However, Sauter Mean Diameter (SMD) as a microscopic property is utilized for appraisement of atomization procedure level. Average diameter of all groups of droplets is the considered definition for SMD value at the calculation time.

However, length of the liquid phase of the injected fuel from the injector nozzle through the jet of the liquid spray to the utmost axial location of the liquid spray boundary is used for measurement of the penetration length. An angle between the two lines starting from the injector's nozzle to two points with maximum radial distance of the liquid parcels is considered for the spray cone angle. Schematic illustration of the liquid spray penetration length and half spray cone angle are presented in Fig. 16.

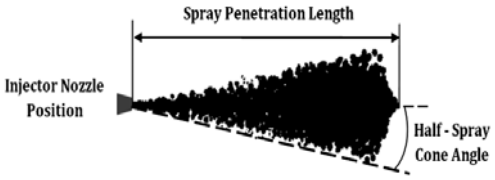


**Fig. 16. Definition of the spray penetration length and half spray cone angle.**

The influences of different blended fuels in comparison with pure HFO on the microscopic and macroscopic spray characteristics are also investigated. Accordingly, spray penetration length, spray cone angle, spray volume, and SMD of the blended fuels and pure HFO are provided in Fig. 17.

Based on Fig. 17 (a), it can be concluded that all blended fuels have longer spray penetration than the pure HFO. This phenomenon can be the result of the decrease in dynamic viscosity and surface tension in the blended fuels (Wang *et al*. 2010; Lefebvre 1989). The growing trend of the blended fuels with linear rate until 0.5 ms and asymptomatic trend after this time is similar to that of pure HFO. Furthermore, negligible smaller spray penetration length is detectable for HFO-normal Butanol compared to two other blended fuels, especially until 1ms. After this time, the penetration lengths of all three blended fuels have approximately similar value. Also, based on Fig. 17(b), spray cone angles of the blended fuels are considerably larger compared to the pure HFO. Also, the spray cone angles for all fuels have a decreasing trend after the start of injection. Moreover, a little larger spray cone angle is detectable for HFO-Ethanol after 1ms. However, before this time, all three blended fuels have approximately the same value.

Due to higher penetration length and spray cone angle for the blended fuels, greater spray volume is anticipated for the blended fuels compared to pure HFO. Based on this forecast and according to Fig.17(c), significant enhancement in spray volume is obtained by the use of the blended fuels instead of the pure HFO. Moreover, HFO-Ethanol has a greater spray volume, especially after 1.5ms. Consequently, these higher values represent a better homogeneity in the air-fuel mixture for the considered blended fuels.

One the other hand, based on Fig. 17(d), the blended fuels have remarkable lower SMD value compared to that of pure HFO. This observation can be attributed to the significant decrease in the surface tension and density value of the blended fuels rather than that of pure HFO. Also, HFO-Ethanol and HFO-Methanol have lower SMD rather than HFO-normal Butanol in accordance with histogram of the particle diameter (Fig. 15).

In addition, it is also evident that SMD value for HFO-Methanol is lower than HFO-Ethanol. However, this difference in SMD is below 1%. Hence, it is not quite visible in Fig.17 (d).

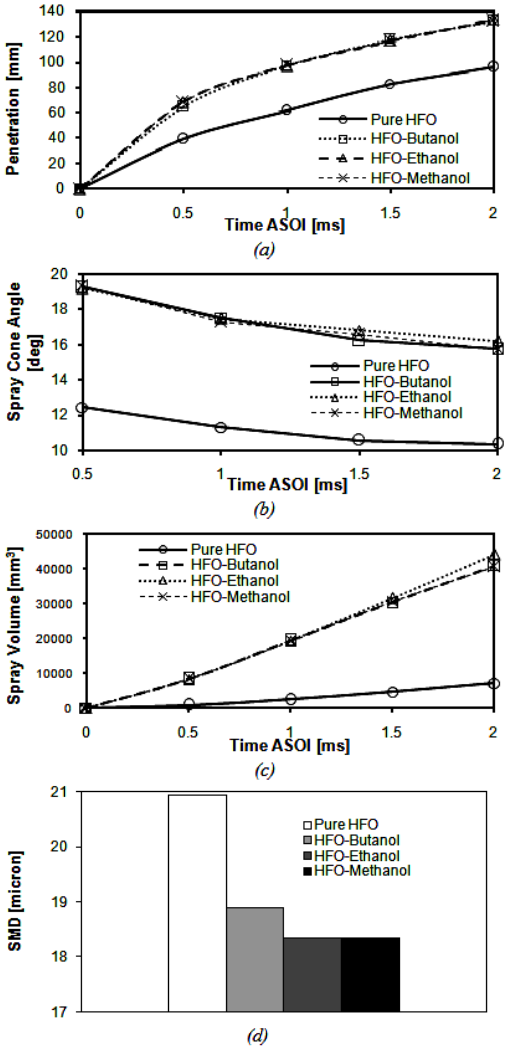


**Fig. 17. a) Spray penetration length, b) spray cone angle, c) spray volume and d) SMD for HFO-normal butanol or ethanol or methanol emulsified fuels.**

Finally, one can conclude that non-reacting spray characteristics are significantly affected by the injected fuel properties. Indeed, small differences in density, viscosity, and surface tension of the injected fuels can have major effects on the injected spray (Lefebvre 1989; Dizayi *et al*. 2014). In other words, based on Lefebvre's (1989) study, viscosity and surface tension increase lead to higher spray penetration length and spray cone angle. However, larger density has an inverse influence on the spray penetration length and spray cone angle (Wang *et al*. 2010; Nishida *et al*. 2007). On the other hand, lower viscosity increases the instabilities required for the injected fuel jet to breakup. This accelerates the atomization procedure and leads to lower SMD. In addition, a decrease in the injected fuel density directly affects the atomization procedure (Ejim *et al*. 2007). Moreover, a higher surface tension acts against the formation of smaller droplets from the liquid fuel (Lefebvre 1989). Consequently, a decrease in surface tension improves the atomization procedure and results in a lower SMD.

## 6. CONCLUSIONS

Addition of alcohols to the basic fuels is an attractive method for controlling the emission instantaneously with improvement in fuel efficiency. Consequently, in the current study, various computational fluid dynamic analyses are preformed for evaluation of non-reacting spray characteristics of the blended fuels. Accordingly, three different blended fuels are considered by blending of HFO with 20% (volumetric percentage) of n-Butanol, Ethanol or Methanol bio-alcohols compared to pure HFO.

For assessment of the spray characteristics, initially the non-dimensional numbers of Weber and Ohnesorge are investigated. Subsequently, through liquid spray morphology, the spray structures for different fuels are evaluated. In addition, histograms of density and droplet diameter of the blended fuels are studied. Finally, the microscopic and macroscopic characteristics of the spray of blended fuels are probed. For this purpose, spray penetration, spray cone angle, spray volume, and SMD criteria are considered.

To accomplish the intended goals of the present study, the OpenFOAM as an open source CFD toolbox is employed. To simulate the interaction of continuous fuel with gaseous medium, the Eulerian-Lagrangian multiphase scheme is implemented. Moreover, by Lagrangian Particle Tracking (LPT) technique, the liquid fuel droplets are tracked. For modeling the turbulence, the standard model of K-ε in RANS is considered. Also, a hybrid breakup model of KH-RT is used for the primary and secondary breakup modeling.

For validation purposes, a mesh resolution sensitivity analysis of HFO is initially conducted. Afterwards, spray penetration and spray cone angle of HFO are validated against experimental data with proper accordance. In addition, the numerical result of spray penetration of butanol under injection pressure of 72 MPa is validated with the reported experiment.

Based on the computational results, higher maximum value is detected in Weber number for the HFO-Ethanol. This result indicates a lower surface tension for HFO-Ethanol compared to other fuels, while larger Ohnesorge number is achieved for HFO-normal Butanol. Based on the liquid spray morphology, the blended fuels have sharper tip. Also, based on the histogram of droplet diameter, an improvement in the breakup procedure of HFO-methanol is concluded compared to the other two blended fuels. This can be attributed to the more frequent data of HFO-methanol in the interval having lower value of droplet diameter.

Finally, higher spray penetration length, spray cone angle, spray volume, and lower SMD is achieved by the use of blended fuels instead of pure HFO. In addition, insignificantly greater value of penetration, spray cone angle, and spray volume are obtained for HFO-Ethanol. That is indicative of the superior macroscopic properties of this fuel compared to other fuels.

## REFERENCES


Andreadis, P., A. Zompanakis, C. Chryssakis and L. Kaiktsis (2011). Effects of the fuel injection parameters on the performance and emissions formation in a large-bore marine diesel engine. *Int. J. Engine. Res. 12(1), 14–29.*

Behringer, M. K. (2014). *Effect of ethanol and butanol content in future fuel blends on spray and combustion characteristics in DISI engines.* Ph.D thesis, University College London, London, UK.

Bellman, R. and R. Pennington (1954). Effects of surface tension and viscosity on Taylor instability. *Q Appl. Math. 12(2), 151–162.*

Can, O., I. Celikten and N. Usta (2004). Effects of addition on performance and emissions of a turbocharged indirect injection diesel engine running at different injection pressures. Energ. Convers. *Manage. 45(15-16), 2429–2440.*

Canakci, M., C. Sayin and M. Gumus (2008). Exhaust emissions and combustion characteristics of a direct injection (DI) diesel engine fueled with methanol–diesel fuel blends at different injection timings. *Energy Fuels 22(6), 3709–3723.*

Chauhan, B. S., N. Kumar, S. S. Pal and Y. D. Jun (2011). Experimental studies on fumigation of ethanol in small capacity diesel engine. *Energy 36(2), 1030–1038.*

Cordtz, R., J. Schramm, A. Andreasen, S. S. Eskildsen and S. Mayer (2013). Modeling the distribution of sulfur compounds in a large two stroke diesel engine. *Energy Fuels 27(3), 1652–1660.*

Dizayi, B., H. Li, A. S. Tomlin and A. Cunliffe (2014). Evaluation of the effect of fuel properties on the fuel spray jet and characteristics in a HGV DI diesel engine operated by used cooking oils. *Applied mechanics and materials 694, 3-12.*

Doˇgan, O. (2011). The influence of n-butanol/diesel fuel blends utilization on a small diesel engine performance and emissions. *Fuel 90(7), 2467–2472.*

Ejim, C. M., B. A. Fleck and A. Amirfazli (2007). .Analytical Study for Atomization of Biodiesels and their Blends in a Typical Injector: *Surface Tension and Viscosity Effects. Fuel 86(10-11), 1534–1544.*

Fink, C., B. Buchholz, M. Niendorf and H. Harndorf (2008). Injection spray analyses from medium speed engines using marine fuels. In Proceedings of the 22nd European Conference on Liquid *Atomization and Spray Systems (ILASS '08), Lake Como, Italy.*

Ghasemi, A., K. Fukuda, R. Balachandar and R. M. Barron (2012). Numerical investigation of spray characteristics of diesel alternative fuels. *SAE Technical Paper, Paper No. 2012- 01-1265.*

Gjesing, R., J. Hattel and U. Fritsching (2009). Coupled atomization and spray modeling in the spray forming process using OpenFOAM. Eng. *Appl. Comp. Fluid. 3(4), 471–486.*

Hwang, S. S., Z. Liu and R. D. Reitz (1996). Breakup mechanisms and drag coefficients of high-speed vaporizing liquid drops. *Atomization Spray 6(3), 353–376.*

Ismail, H. M., H. K. Ng, S. Gan and T. Lucchini (2013). Computational study of biodiesel-diesel fuel blends on emission characteristics for a light-duty diesel engine using OpenFOAM. *Appl. Energ. 111, 827–841.*

Jiang, X., G. A. Siamas, K. Jagus and T. G. Karayiannis (2010). Physical modeling and advanced simulations of gas-liquid two-phase jet flows in atomization and sprays. *Prog. Energ. Combust. 36(2), 131–167.*

Karabektas, M. and M. Hosoz (2009). Performance and emission characteristics of a diesel engine using isobutanol-diesel fuel blends. *Renew. Energ. 34(6), 1554–1559.*

Kassem, H. I., K. M. Saqr, H. S. Aly, M. M. Sies and M. A. Wahid (2011). Implementation of the eddy dissipation model of turbulent non-premixed combustion in OpenFOAM. Int. Commun. *Heat. Mass. 38(3), 363–367.*

Kumar, S., J. H. Cho, J. Park and I. L. Moon (2013). Advances in diesel-alcohol blends and their effects on the performance and emissions of diesel engines. *Renew. Sust. Energ. Rev. 22, 46–72.*

Kyriakides, N., C. Chryssakis and L. Kaiktsis (2009). Influence of heavy fuel properties on spray atomization for marine diesel engine applications. *SAE Technical Paper, Paper No. 2009-01-1858.*

Lefebvre, A. H. (1989). *Atomization and sprays*. Hemisphere Publishing Corporation, New York, USA.

Nishida, K., W. Zhang and T. Manabe (2007). Effects of micro-hole and ultra-high injection pressure on mixture properties of D.I. diesel spray. *SAE Technical Paper No. 2007-01-1890.*

Nowruzi, H., P. Ghadimi and M. Yousefifard (2014). A numerical study of spray characteristics in medium speed engine fueled by different HFO/n-butanol blends. *International Journal of Chemical Engineering, 1-12.*

Park, S. H., I. M. Youn and C. S. Lee (2010). Influence of two-stage injection and exhaust gas recirculation on the emissions reduction in an ethanol-blended diesel-fueled four-cylinder diesel engine. *Fuel Process. Technol. 91(11), 1753–1760.*

Park, S. H., J. Cha and C. S. Lee (2010). Effects of

bioethanol-blended diesel fuel on the combustion and emission reduction characteristics in a direct-injection diesel engine with exhaust gas recirculation (EGR). *Energy Fuels 24(7), 3872–3883.*

Pickett, L., J Manin, R. Payri, M. Bardi and J. Gimeno (2013). Transient rate of injection effects on spray development. *SAE Technical Paper, Paper No. 2013-24-0001.*

Rakopoulos, D. C., C. D. Rakopoulos, E. G. Giakoumis, A. M. Dimaratos and D. C. Kyritsis (2010). Effects of butanol–diesel fuel blends on the performance and emissions of a high-speed di diesel engine. *Energ. Convers. Manage. 51(10), 1989–97.*

Reddemann, M. A., F. Mathieu, D. Martin and R. Kneer (2009). Experimental investigation of spray propagation and mixture formation of Tailor-made fuels under engine-relevant conditions. *In Proceedings of the 11th Triennial International Annual Conference on Liquid Atomization and Spray Systems (ICLASS'09), Vail, Colorado, USA, 26-30.*

Reitz, R. D. (1987). Modeling atomization processes in high pressure vaporizing sprays. *Atomisation and Spray Technology 3(4), 309–337.*

Reitz, R. D. and J. R. Diwakar (1986). Effect of drop break-up on fuel sprays. *SAE Technical Paper, Paper No.860469.*

Reitz, R. D. and J. R. Diwakar (1987). Structure of high-pressure fuel sprays. SAE Technical Paper, Paper No.870598.

Sayan, C., A. N. Ozsezen and M. Canakci (2010). The influence of operating parameters on the performance and emissions of a di diesel engine using methanol- blended-diesel fuel. *Fuel 89(7), 1407–1414.*

Sayin, C., M. lhan, M. Canakci and M. Gumus (2009). Effect of injection timing on the exhaust emissions of a diesel engine using diesel–methanol blends. *Renew. Energ. 34(5), 1261–1269.*

Sepret, V., R. Bazile and M. Marchal (2010). Effect of ambient density and orifice diameter on gas entrainment by a single-hole diesel spray. *Exp. Fluids. 49, 1293-1305.*

Song, R., J. Liu, L. Wang and S. Liu (2008). Performance and emissions of a diesel engine fueled with methanol. *Energy Fuels 22(6), 3883–3888.*

Stamoudis, N., C. Chryssakis and L. Kaiktsis (2014). A two-component heavy fuel oil evaporation model for CFD studies in marine diesel engines. *Fuel 115, 145–153.*

Struckmeier, D., D. Tsuru, S. Kawauchi and H. Tajima (2009). Multicomponent modeling of evaporation, ignition and combustion processes of heavy residual fuel oil. *In Proceedings of the SAE International Powertrains, Fuels and Lubricants Meeting, Florence, Italy.*

Tsang, K. S., Z. H. Zhang, C. S. Cheung and T. L. Chan (2010). Reducing emissions of a diesel engine using fumigation ethanol and a diesel oxidation catalyst. *Energy Fuels 24(11), 6156–6165.*

Wang, H., A. B. Dempsey, M. Yao, M. Jia, and R. D. Reitz (2014). Kinetic and numerical study on the effects of Di-tert-butyl peroxide additive on the reactivity of methanol and ethanol. *Energy Fuels 28(8), 5480–5488.*

Wang, X., Z. Huang, O. A. Kuti, W. Zhang and K. Nishida (2010). Experimental and analytical study on biodiesel and diesel spray characteristics under ultra-high injection pressure. *Int. J. Heat. Fluid. Fl. 31(4), 659–666.*

Yao, M., Wang, H., Zheng, Z. and Y. Yue (2010). Experimental study of n-butanol additive and multi-injection on hd diesel engine performance and emissions. *Fuel 89(9), 2191–201.*

Yoon, S. H., S. H. Park, H. K. Suh and C. S. Lee (2011). Effect of biodiesel-ethanol blended fuel spray characteristics on the reduction of exhaust emissions in a common-rail diesel engine. *J. Energy Resour. Technol. 132(4), 1-7.*

Yousefifard, M., P. Ghadimi and H. Nowruzi (2014). three-dimensional LES modeling of induced gas motion under the influence of injection pressure and ambient density in an ultrahigh-pressure diesel injector. *J. Braz. Soc. Mech. Sci.*

Yousefifard, M., P. Ghadimi and H. Nowruzi (2015). Numerical investigation of the effects of chamber backpressure and temperature on HFO spray characteristics. *Int. J. Automot. Techn. 16(2), 339−349.*

Zhang, Z. and R. Balasubramanian (2014). Influence of butanol-diesel blends on particulate emissions of a non-road diesel engine. *Fuel 118, 130–136.*

Zhang, Z. H., K. S. Tsang, C. S. Cheung, T. L. Chan and C. D. Yao (2011). Effect of fumigation methanol and ethanol on the gaseous and particulate emissions of a direct-injection diesel engine. *Atmos. Environ. 45(11), 2001–2008.*

Zoulalian, A. (2010). Biomass position for renewable energies: main ways of energetic valorization. *Journal of Applied Fluid Mechanics. 3(1), 47-54.*